Progress In Electromagnetics Research Letters, Vol. 22, 19–28, 2011

NARROWBAND FREQUENCY SELECTIVE SURFACE BASED ON SUBSTRATE INTEGRATED WAVEGUIDE TECHNOLOGY

H. Zhou, S. Qu, Z. Pei, J. Zhang, B. Lin, J. Wang, H. Ma and C. Gu

College of Science
Air Force Engineering University, Xi'an 710051, China

Z. Xu

Electronic Materials Research Laboratory
Key Laboratory of the Ministry of Education
Xi'an Jiaotong University, Xi'an 710049, China

P. Bai and W. Peng

Synthetic Electronic Information System Research Department
Air Force Engineering University, Xi'an 710051, China

Abstract—In this paper, a novel narrowband frequency selective surface (FSS) with a stable performance based on substrate integrated waveguide technology is presented. The unit cell of the FSS consists of a double-sided metalized substrate with a circular hole and a SIW circular cavity. In this way, incident EM waves enter the circular cavity and excite a TM_{110} cavity resonance, leading to a narrow pass-band. The high-Q property of the TM_{110} cavity resonance provides a very good wide-angle and polarization-independent stability. Both the simulation and experimental results show that such narrowband FSS owes its advantages to high selectivity, low profile stable performance with various incident angles and different polarizations, which is suitable for impulse detections, narrow-band communications, electronic countermeasures, etc.

Received 20 February 2011, Accepted 15 March 2011, Scheduled 23 March 2011
Corresponding author: Hang Zhou (zh_cn1120@163.com)).

1. INTRODUCTION

For more than four decades, Frequency Selective Surfaces (FSSs) have been widely studied for their various applications in spatial microwave and optical filters. They have been used as polarizers, filters, subreflectors, band-pass hybrid radomes for radar cross section (RCS) controlling [1]. In these applications, it is necessary that FSS provide stable performance for different incidence angles and polarization states. Many methods are adopted to improve the performance of FSSs. Luebbers and Munk studied the effects of dielectric loading on FSSs [2]. Three-dimensional structures were designed to obtain isotropic FSSs [3]. Complementary FSSs have been analyzed in [4–6]. References [7–10] made use of resonant structures to design miniaturized FSSs whose dimensions were much smaller than the operating wavelength. In order to get high quality factor of open resonance structures, substrate integrated waveguide (SIW) technology was introduced by Luo et al. [11] to design high performance FSSs. SIW-FSS structures keep the advantages of conventional metallic waveguides, such as high Q-factor, high selectivity, cutoff frequency characteristic, high power capacity etc. Based on this method, many excellent SIW-FSSs were studied in [12–14].

In some practical applications, such as impulse detections, electronic countermeasures, narrowband communications, narrowband FSSs are required to improve the out-of-band block performance, or to increase the utility and re-use of the available spectrum. Single and two layer FSSs with narrow passband have been studied in [15] and [16], respectively. Parker et al. studied two arrays of single-ring slots with different radii supported on either side of a thin dielectric substrate form FSS with narrow band-pass transmission responses [17]. Design of narrow band-pass waveguide filter using FSSs loaded with surface mount capacitors based on split-field update FDTD method was reported in [18]. In [19], the Fabry-Perot approach is introduced to design narrow band-pass FSSs.

In this paper, we use the SIW technology to design a narrow band-pass FSS. The resonance introduced by the cavity possess a stable performance whatever the incident angles or the polarizations are. The aperture resonance is adjusted to be far away from the cavity resonance in order not to disturb the cavity resonance. In the end, we obtained a narrow band-pass frequency selective surface with excellent performances. Both the simulation and experimental results show that this narrowband FSS has advantages of high selectivity, stable performance, compact volume and it is easy to be fabricated by the print circuit board (PCB) technology without post processes.

2. ANALYSIS AND DESIGN

Geometrical dimensions of the unit cell in Fig. 1 are: $p = 15\,\text{mm}$, $d_0 = 4.8\,\text{mm}$, $d_1 = 1.0\,\text{mm}$, $d_2 = 0.2\,\text{mm}$. $r_c = 6.8\,\text{mm}$, $\theta = pi/12$. In order to form SIW cavity whose quality factor is no less than that of conventional metal cavity, the conditions of $d_1/\lambda_0 \leq 0.1$ and $d_1/(b^*\gamma) \geq 0.5$ must be satisfied [20], so we chose $d_1 = 1\,\text{mm}$, $\theta = pi/12$. 24 metallic stubs are arranged so as to form a circular waveguide cavity. The FSS arrays have a substrate with relative permittivity of $\varepsilon_r = 2.65$, loss tangent of 0.001 and thickness of $h_{sub} = 1\,\text{mm}$. A hole with diameter $d_0 = 4.8\,\text{mm}$ was punched through the substrate. Such periodic distribution of sub-wavelength hole could lead to extraordinary transmission phenomenon which has been fully studied and experimentally verified in [21–24]. In this paper, we will observe the relative field distributions to analyse this phenomenon.

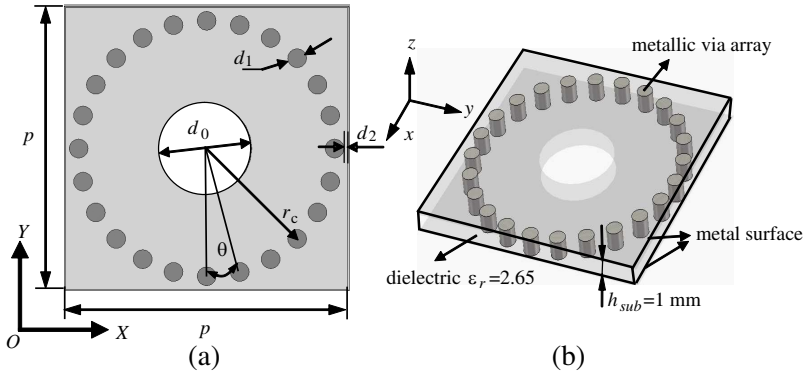

Figure 1. Geometrical configuration of the unit cell. (a) Top view. (b) 3D view

We used the full wave simulation method finite element method (FEM) to calculate its reflection and transmission characteristics. Assume that the SIW-FSS is an infinite periodic structure. The single SIW-FSS is excited by an incident plane wave with different incident angles and polarizations. The four sides of the unit cell are set to be periodic boundary conditions (PBC). Fig. 2 gives the transmission spectra under normal incidence. We can see from Fig. 2 that there are three evident resonances at 16.6 GHz, 30.4 GHz and 34.4 GHz, respectively.

The electric field distributions at the first resonance at 16.6 GHz are plotted in Fig. 3(a). The first resonance at 16.6 GHz corresponds to a cavity resonance introduced by the circular SIW cavity. The

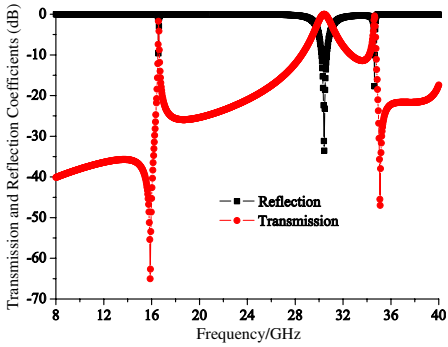

Figure 2. Simulated frequency response of the structure.

electric field component is mainly Ez and it is perpendicular to the incident plane as well as the incident field, as shown under the Fig. 3(a). Fig. 3(b) gives the magnetic field distribution at 16.6 GHz under normal incidence. It can be found that the magnetic field at 16.6 GHz exhibits two vortex-like magnetic fields with opposite directions. So we can affirm that it is a TM_{110} cavity mode which is similar to that of a conventional circular cavity resonance.

The second at 30.4 GHz corresponds to an aperture resonance, since the main electric field component is Ey, which is along the aperture, as shown in Fig. 3(c). The third resonance at 34.4 GHz is a higher-order cavity resonance. It is a TM_{120} mode and the main electric field component is Ez, which is also perpendicular to the incident field, as shown in Fig. 3(d).

3. FSS WITH STABLE RESONANCE

It is necessary that FSS provide stable performance under different incidence angles and polarizations. Usually, slot FSS based on SIW cavity are constructed to get two resonances and then the two resonances are adjusted so as to be close to each other. A transmission null is caused by the coupling effect of the two resonances. A rapid roll-off edge will be generated by this transmission null. So a FSS with high selectivity and stable performance will be obtained [11]. Furthermore, multilayer and component FSS-SIW structures are cascaded to obtain quasi-elliptic band-pass response [12, 14].

In this paper, we do not concern the aperture's resonance and higher-order resonances of the cavity, but just focus on the SIW cavity resonance. Fig. 4 gives the frequency responses under different incidence angles and polarizations. From Fig. 4 we can find that

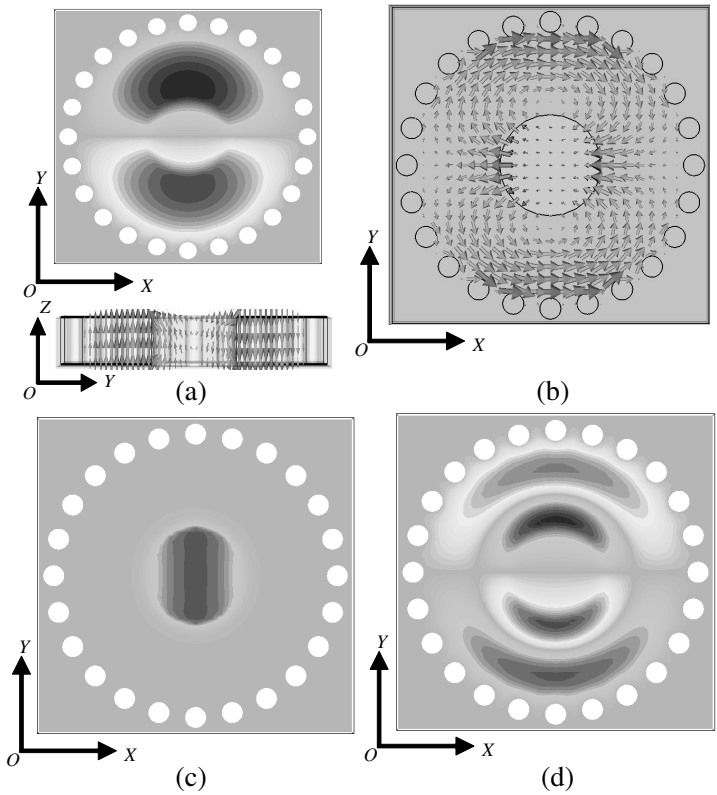

Figure 3. Field distribution diagrams of different modes in which the white blank corresponds to zero electric field and black corresponds to the strongest electric field. (a) Electric field distribution diagrams of the cavity TM_{110} resonance. (b) Magnetic field distribution diagrams of cavity TM_{110} resonance. (c) Aperture resonance at 30.4 GHz. (d) Higher-order cavity resonance at 34.4 GHz.

frequency of TM_{110} cavity resonance is rather stable under oblique incidence angles from 0° to 50° for both TE and TM polarization. The aperture resonance frequencies shift from 30.4 GHz to 29.1 GHz (TM polarization)/28.8 GHz (TE polarization) as the incident angles increase from 0° to 50°. For both TM and TE polarizations, the higher order cavity resonances frequencies decrease from 34.4 GHz to 34.0 GHz as the incident angles increase from 0° to 50°. Grating lobes emerged at about 39.0 GHz for TM polarization at 25° incident angle. When the incident angle increases to 50°, the grating lobes shift to 33.0 GHz. For TE polarization and 25° incident angle, grating lobes emerge

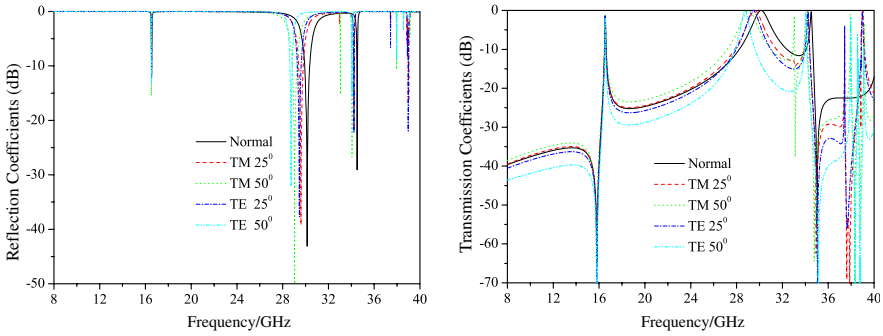

Figure 4. Frequency responses of the FSS with different polarizations and incident angles. (a) Reflection. (b) Transmission.

at 38.9 GHz. When the incident angle increases to 50°, the grating lobes shift to 37.4 GHz. The desired central resonance frequency is at 16.6 GHz and the −0.5 dB and −3 dB bandwidth are 16 MHz, 51 MHz, respectively. So the associated loaded quality factor is about 325.5. The bandwidth ratio of different polarizations and different incident angles is very close to 1.0. In addition, even up to 28 GHz, there are no other resonance frequencies or grating lobes.

4. EXPERIMENT

An experiment was carried out to verify our design. The proposed FSS in Section 2 is fabricated by using a F4B-2 substrate, whose permittivity is 2.65 and loss tangent 0.001. Fig. 5(a) shows the prototype of the fabricated structure. It is made up of the array of 15×15 (in the x- and y-axis directions) unit cells, so the overall size of the structure is 225 mm × 225 mm. The FSS was measured by free space method.

Measured and simulated transmission coefficients with a plane wave normal incidence are presented in Fig. 5(b). The measured insertion loss of 1.4 dB is higher than the simulated insertion loss of 1.2 dB. Measured resonance frequencies shift from 16.6 GHz (simulation ones) to 16.9 GHz. Such discrepancies between the measured and simulated results can mainly be attributed to fabrication precision of the structure and the losses of the measuring system. Figs. 5(c) and (d) show the measured transmission spectra under different incident angles at TE polarization and TM polarization, respectively. Because the sample is not large enough, edge effect will

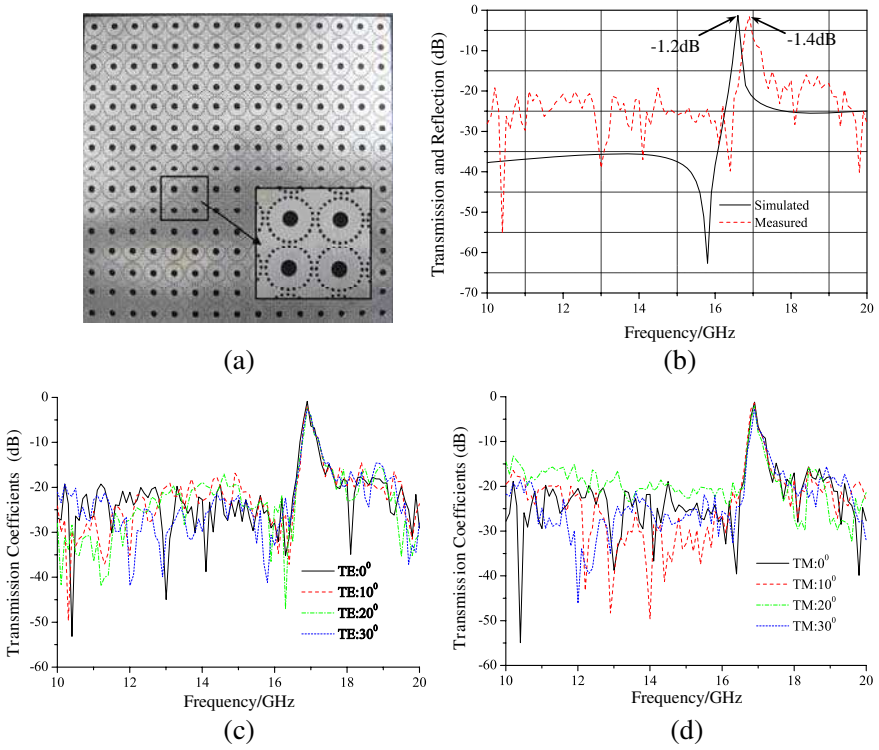

Figure 5. Experiment. (a) Prototype of the fabricated structure. (b) Simulated and measured results comparison with plane wave normal incidence. (c) Measured transmission curves with various incident angles with TE polarization. (d) Measured transmission curves with various incident angles with TM polarization.

be caused as the incident angle increases, so the incident angles in the measurement are limited below 30°. Because of the symmetry of SIW cavity FSS, the frequency response of the two different polarizations under normal incidence is identical in theory.

The measure resonant frequencies occur at 16.90 GHz are not changed not only under various incidence angles but also at different polarizations. Insertion loss increases slightly as the incident angles increase. Bandwidth ratio of different polarizations and different incident angles is still near 1.0. In addition, there are no other transmission resonance frequencies except the expected ones.

5. CONCLUSION

In this paper, we proposed a novel compact frequency selective surface with stable frequency-selective performances. The cavity resonance provides excellent stability to both oblique incidences and different polarizations. An experiment was carried out. The measured results are in good agreement with the simulation ones. The narrow pass-band FSS has advantages of high selectivity, quite stable performance and its thickness is less than $\lambda/18$. The presented FSS, by virtue of these advantages, provides practical applications to impulse detections, narrow-band communications, electronic countermeasures, etc.

ACKNOWLEDGMENT

This project is supported partly by the National Natural Science Foundation of China under Grants 50632030, 60871027, 60901029 and in part by the National Basic Research Program of China (Grant No. 2009CB623306).

REFERENCES

1. Munk, B. A., *Frequency Selective Surfaces: Theory and Design*, Wiley, New York, 2000.
2. Luebbers, R. J. and B. A. Munk, "Some effects of dielectric loading on periodic slot arrays," *IEEE Trans. Antennas Propag.*, Vol. 26, No. 4, 536–542, Jul. 1978.
3. Baena, J. D., L. Jelinek, R. Marqués, J. J. Mock, J. Gollub, and D. R. Smith, "Isotropic frequency selective surfaces made of cubic resonators," *Appl. Phys. Lett.*, Vol. 91, 191105, 2007.
4. Wakabayashi, H., M. Kominami, H. Kusaka, and H. Nakashima, "Numerical simulations for frequency-selective screens with complementary elements," *IEE Proc. — Micro. Antennas Propag.*, Vol. 141, No. 6, 477–482, 1994.
5. Lockyers, D. S., J. C. Vardaxpglou, and R. A. Simpkin, "Complementary frequency selective surfaces," *IEE Proc. — Micro. Antennas Propag.*, Vol. 147, No. 6, 501–507, 2000.
6. Hu, X.-D., X.-L. Zhou, L.-S. Wu, L. Zhou, and W.-Y. Yin, "A miniaturized dual-band frequency selective surface (FSS) with closed loop and its complementary pattern," *IEEE Antennas Wireless Propag. Lett.*, Vol. 8, 1374–1377, 2009.
7. Sarabandi, K. and N. Behdad, "A frequency selective surface with

miniaturized elements," *IEEE Trans. Antennas Propag.*, Vol. 55, No. 5, 1239–1245, 2007.

8. Bayatpur, F. and K. Sarabandi, "Single-layer, high-order, miniaturized element requency selective surfaces," *IEEE Trans. Microw. Theory Tech.*, Vol. 56, No. 4, 774–781, Apr. 2008.
9. Chiu, C.-N. and K.-P. Chang, "A novel miniaturized-element frequency selective surface having a stable resonance," *IEEE Antennas Wireless Propag. Lett.*, Vol. 8, 1175–1177, 2009.
10. Bayatpur, F. and K. Sarabandi, "Miniaturized FSS and patch antenna array coupling for angle-independent, high-order spatial filtering," *IEEE Microw. Wireless Compon. Lett.*, Vol. 20, No. 2, 79–81, 2010.
11. Luo, G. Q., W. Hong, Z. C. Hao, B. Liu, W. D. Li, et al., "Theory and experiment of novel frequency selective surface based on substrate integrated waveguide technology," *IEEE Trans. Antennas Propag.*, Vol. 53, No. 12, 4035–4043, Dec. 2005.
12. Luo, G. Q., W. Hong, Q. H. Lai, K. Wu, and L. L. Sun, "Design and experimental verification of compact frequency-selective surface with quasi-elliptic bandpass response," *IEEE Trans. Microw. Theory Tech.*, Vol. 55, No. 12, 2481–2487, 2007.
13. Luo, G. Q., W. Hong, H. J. Tang, J. X. Chen, and L. L. Sun, "Triband frequency selective with periodic cell perturbation," *IEEE Microw. Wireless Compon. Lett.*, Vol. 17, No. 6, 2007.
14. Yang, H.-Y., S.-X. Gong, P.-F. Zhang, and Y. Guan, "Compound frequency selective surface with quasi-elliptic bandpass response," *Electron. Lett.*, Vol. 45, No. 1, 2010.
15. Lima, A. C. De C. and E. A. Parker, "Narrow bandpass single layer frequency selective surfaces," *Electron. Lett.*, Vol. 29, No. 8, 1993.
16. Lockyer, D. S. and J. C. Vardaxoglou, "Reconfigurable FSS response from two layers of slotted dipole arrays," *Electron. Lett.*, Vol. 32, No. 6, 1996.
17. Parker, E. A. and A. Stanley, "Dual-polarized narrow-bandpass frequency-selective surfaces," *Microw. Opt. Techn. Lett.*, Vol. 13, 105–107,1996.
18. Mohammad Amjadi, S. and M. Soleimani, "Design of band-pass waveguide filter using frequency selective surfaces loaded with surface mount capcitors based on split-field update FDTD method," *Progress In Electromagnetics Research B*, Vol. 3, 271–281, 2008.
19. Zhang, J.-C., Y.-Z. Yin, and J.-P. Ma, "Design of narrow band-

pass frequency selective surface for millimeter wave applications," *Progress In Electromagnetics Research*, Vol. 96, 287–298, 2009.

20. Zhang, Y. L., W. Hong, K. Wu, J. X. Chen, and H. J. Tang, "Novel substrate integrated waveguide cavity filter with defected ground structure," *IEEE Trans. Microw. Theory Tech.*, Vol. 53, No. 4, 2005.
21. Medina, F., F. Mesa, and R. Marqus, "Extraordinary transmission through arrays of electrically small holes from a circuit theory perspective," *IEEE Trans. Microw. Theory Tech.*, Vol. 56, No. 12, 3108–3120, 2008.
22. Medina, F., F. Mesa, J. A. Ruiz-Cruz, J. M. Rebollar, and J. R. Montejo-Garai, "Study of extraordinary transmission in a circular waveguide System," *IEEE Trans. Microw. Theory Tech.*, Vol. 58, No. 6, 1532–1542, 2010.
23. Kontogeorgos, A. A., D. P. korfiatis, K. A. T. Thoma, and J. C. Vardaxoglou, "plasma generation in silicon based inductive grid arrays," *Optics and Lasers in Engineering*, Vol. 47, No. 11, 1195–1198, 2009.
24. Doumanis, E. T., J. C. Vardaxoglou, D. P. Korfilatis, and K. A. T. Thoma, "Integrated Schottky-contact in 2-layer inductive grid array," *The Second European Conference on Antennas and Propagation*, 1–6, 2007.